Considerations on the electromagnetic flow in Airy beams based on the Gouy phase

Carlos J. Zapata-Rodríguez,[1,*] **David Pastor,**[1] **and Juan J. Miret**[2]

[1]*Department of Optics, University of Valencia, Dr. Moliner 50, 46100 Burjassot, Spain*
[2]*Department of Optics, Pharmacology and Anatomy, University of Alicante, Spain*

**carlos.zapata@uv.es*

Abstract: We reexamine the Gouy phase in ballistic Airy beams (AiBs). A physical interpretation of our analysis is derived in terms of the local phase velocity and the Poynting vector streamlines. Recent experiments employing AiBs are consistent with our results. We provide an approach which potentially applies to any finite-energy paraxial wave field that lacks a beam axis.

OCIS codes: (070.7345) Wave propagation; (260.1960) Diffraction theory; (350.5030) Phase.

References and links

1. L. G. Gouy, "Sur une propriété nouvelle des ondes lumineuses," Compt. Rendue Acad. Sci. (Paris) **110**, 1251–1253 (1890).
2. S. Feng and H. G. Winful, "Physical origin of the Gouy phase shift," Opt. Lett. **26**, 485–487 (2001).
3. T. D. Visser and E. Wolf, "The origin of the Gouy phase anomaly and its generalization to astigmatic wavefields," Opt. Commun. **283**, 3371–3375 (2010).
4. R. W. Boyd, "Intuitive explanation of the phase anomaly of focused light beams," J. Opt. Soc. Am. **70**, 877–880 (1980).
5. A. E. Siegman, *Lasers* (University Science Books, Mill Valley, 1986).
6. G. G. Paulus, F. Lindner, H. Walther, A. Baltuska, E. Goulielmakis, M. Lezius, and F. Krausz, "Measurement of the phase of few-cycle laser pulses," Phys. Rev. Lett. **91**, 253004 (2003).
7. A. Apolonski, P. Dombi, G. Paulus, M. Kakehata, R. Holzwarth, T. Udem, C. Lemell, K. Torizuka, J. Burgdörfer, T. Hänsch, and F. Krausz, "Observation of light-phase-sensitive photoemission from a metal," Phys. Rev. Lett. **92**, 073902 (2004).
8. X. Pang, G. Gbur, and T. D. Visser, "The Gouy phase of Airy beams," Opt. Lett. **36**, 2492–2494 (2011).
9. G. A. Siviloglou and D. N. Christodoulides, "Accelerating finite energy Airy beams," Opt. Lett. **32**, 979–981 (2007).
10. M. A. Bandres, "Accelerating beams," Opt. Lett. **34**, 3791–3793 (2009).
11. Y. Hu, G. Siviloglou, P. Zhang, N. Efremidis, D. Christodoulides, and Z. Chen, "Self-accelerating Airy beams: generation, control, and applications," in *Nonlinear Photonics and Novel Optical Phenomena*, Z. Chen and R. Morandotti, eds. (Springer, 2012), vol. 170, pp. 1–46.
12. J. Baumgartl, M. Mazilu, and K. Dholakia, "Optically mediated particle clearing using Airy wavepackets," Natura Photon. **2**, 675–678 (2008).
13. P. Polynkin, M. Kolesik, J. V. Moloney, G. A. Siviloglou, and D. N. Christodoulides, "Curved plasma channel generation using ultraintense Airy beams," Science **324**, 229–232 (2009).
14. A. Chong, W. H. Renninger, D. N. Christodoulides, and F. W. Wise, "Airy-Bessel wave packets as versatile linear light bullets," Nat. Photonics **4**, 103–106 (2010).
15. L. Li, T. Li, S. M. Wang, C. Zhang, and S. N. Zhu, "Plasmonic Airy Beam generated by in-plane diffraction," Phys. Rev. Lett **107**, 1–4 (2011).
16. A. Minovich, A. E. Klein, N. Janunts, T. Pertsch, D. N. Neshev, and Y. S. Kivshar, "Generation and near-field imaging of Airy surface plasmons," Phys. Rev. Lett **107**, 116802 (2011).
17. P. Zhang, S. Wang, Y. Liu, X. Yin, C. Lu, Z. Chen, and X. Zhang, "Plasmonic Airy beams with dynamically controlled trajectories," Opt. Lett. **36**, 3191–3193 (2011).

#172359 - $15.00 USD Received 10 Jul 2012; revised 6 Aug 2012; accepted 6 Aug 2012; published 28 Sep 2012

18. W. Liu, D. N. Neshev, I. V. Shadrivov, A. E. Miroshnichenko, and Y. S. Kivshar, "Plasmonic Airy beam manipulation in linear optical potentials," Opt. Lett. **36**, 1164–1166 (2011).
19. M. Born and E. Wolf, *Principles of Optics*, 7th (expanded) ed. (Cambridge University Press, 1999).
20. H. I. Sztul and R. R. Alfano, "The Poynting vector and angular momentum of Airy beams," Opt. Express **16**, 9411–9416 (2008).
21. M. A. Porras, C. J. Zapata-Rodríguez, and I. Gonzalo, "Gouy wave modes: undistorted pulse focalization in a dispersive medium," Opt. Lett. **32**, 3287–3289 (2007).
22. C. J. Zapata-Rodríguez and M. A. Porras, "Controlling the carrier-envelope phase of few-cycle focused laser beams with a dispersive beam expander," Opt. Express **16**, 22090–22098 (2008).

1. Introduction

It is well-known that finite-energy 2D wave fields propagating in free space undergo an overall phase shift of $\pi/2$ rads (π rads for 3D waves) if they are compared with the transit of untruncated plane waves. For aberration-free focused waves, Gouy first realized that the phase is delayed within its focal region [1]. The origin of the Gouy phase (GP) shift is ascribed to the spatial confinement of the optical beam [2, 3], which leads to deviations in the wave front and, therefore, local alterations of the wavenumber in the near field [4, 5]. The interest in the analysis of this effect persists nowadays because of its implication in many ultrafast phenomena that are dependent directly on the electric field rather than the pulse envelope such as electron emission from ionized atoms [6] and metal surfaces [7].

Recently Pang *et al.* studied the phase behavior of Airy beams (AiBs) [8]. Because of its curved trajectory [9, 10], they defined the GP of an AiB as the difference between its phase and that of a diverging cylindrical wave, the latter considered a suitable reference field. In this Paper we reexamine the GP in AiBs. A physical interpretation of the GP is given in terms of the local phase velocity and the Poynting vector streamlines of AiBs. Potential applications of our results to recent experiments employing AiBs [11] are also outlined. They include optical manipulation of small particles [12], generation of curved plasma channels in air [13, 14], and generation of surface plasmons with parabolic trajectories [15–18], to mention a few.

2. Formalism

Let us consider a $(1+1)$D wave field $\exp(ik_0 z)\,u$ which evolves along the z-axis with a carrier spatial frequency $k_0 = \omega/c$. Thus the wave function u satisfies the paraxial wave equation $2i\partial_\zeta u + \partial_{ss} u = 0$ expressed in terms of the normalized spatial coordinates $s = x/w_0$ and $\zeta = z/z_R$. Here w_0 is the beam width and $z_R = k_0 w_0^2$ denotes the propagation distance. Specifically, an AiB may be written as [9]

$$\begin{aligned} u(s,\zeta) &= Ai\left(s - \zeta^2/4 + ia\zeta\right)\exp\left(as - a\zeta^2/2\right) \\ &\quad \times \exp\left(is\zeta/2 + ia^2\zeta/2 - i\zeta^3/12\right), \end{aligned} \tag{1}$$

where $Ai(\cdot)$ denotes the Airy function. The parameter $0 < a \leq 1$ is introduced in the wave function in order to provide $\int |u|^2 ds < \infty$ allowing the paraxial beam to carry a finite energy, and concurrently conserving a central lobe with parabolic shape.

Topologic attributes of AiBs may be drawn without difficulty from its transverse spatial frequency

$$\tilde{u}(k) = \exp\left(-ak^2 + a^3/3 - ia^2 k + ik^3/3\right). \tag{2}$$

Equation (1) is directly derived from the Fresnel-Kirchhoff (FK) diffraction integral $u = (2\pi)^{-1}\int \tilde{u}(k)\exp(i\psi)\,dk$, being $\psi = ks - k^2\zeta/2$ the phase distribution of a plane-wave spectral component with transverse spatial frequency k. The phase $\tilde{\phi} + \psi$ of the integrand is highly

#172359 - $15.00 USD Received 10 Jul 2012; revised 6 Aug 2012; accepted 6 Aug 2012; published 28 Sep 2012

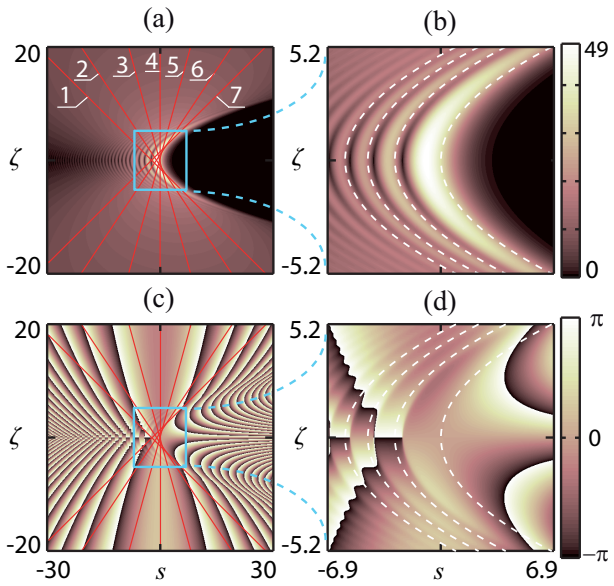

Fig. 1. (a) $|u|$ and (c) ϕ for an AiB with $a = 0.1$. The parabolic curves (4) are drawn in the near field (b) and (d) in dashed lines. In the far field, the numbered straight trajectories of light rays satisfy Eq. (3).

oscillating, where $\tilde{\phi} = \arg(\tilde{u})$. However it reaches a stationary point, that is $\partial_k[\tilde{\phi} + \psi] = 0$, for two frequencies $k_\pm$ satisfying

$$k^2 - k\zeta + s - a^2 = 0. \tag{3}$$

The principle of stationary phase [19] (PSP) establishes that the FK diffraction integral has a predominant contribution of frequencies in the vicinities of $k_\pm$. Inside the geometrical shadow $s > a^2 + \zeta^2/4$ no stationary points may be found. In the light area, constructive interference is attained if the phase $\tilde{\phi} + \psi$ at frequencies k_+ and k_- differs by an amount $2\pi m$, where m is an integer. This condition provides the locus of points with peaks in intensity, which leads to

$$s = a^2 - (3\pi m/2)^{2/3} + (\zeta/2)^2, \text{ for } m \geq 0. \tag{4}$$

These curves describe perfect parabolas.

From geometrical grounds, the parameter k represents a particular light "ray" with linear trajectory (3) in the $s\zeta$-plane. The envelope (caustic) of this family of rays results from the solution given in Eq. (4) for $m = 0$, providing the ballistic signature of an AiB.

In Fig. 1 we show the spatial distribution of the magnitude $|u|$ and the phase $\phi = \arg(u)$ of the wave function given in Eq. (1) corresponding to an AiB of $a = 0.1$. The accelerating behavior of the AiB is limited, and out of the near field the interference-driven parabolic peaks fade away. To establish the boundaries of the near field, we point out that $|\tilde{u}|$ falls off less than a half of its maximum in the interval $k^2 < k_{max}^2 = (\ln 2)/a$, which represents the effective bandwidth of the AiB. Moreover, k_{max} is no more than the far field beam angle in the normalized coordinates, and $k_{max} = 2.6$ in Fig. 1. As a consequence, the length of the caustic is finite and it is observed in $|\zeta| < 2k_{max}$. Along the beam waist $\zeta = 0$ the energy is mostly localized in the region $a^2 - k_{max}^2 \leq s \leq a^2$. In Fig. 1 the near field is bounded within the region $|\zeta| < 5.2$ and $|s| < 6.9$, where 4 interference peaks are clearly formed.

We point out that the maximum of intensity is not placed exactly at points that belong to the curves (4) but they are slightly shifted to lower values of the transverse spatial coordinate s.

#172359 - $15.00 USD Received 10 Jul 2012; revised 6 Aug 2012; accepted 6 Aug 2012; published 28 Sep 2012

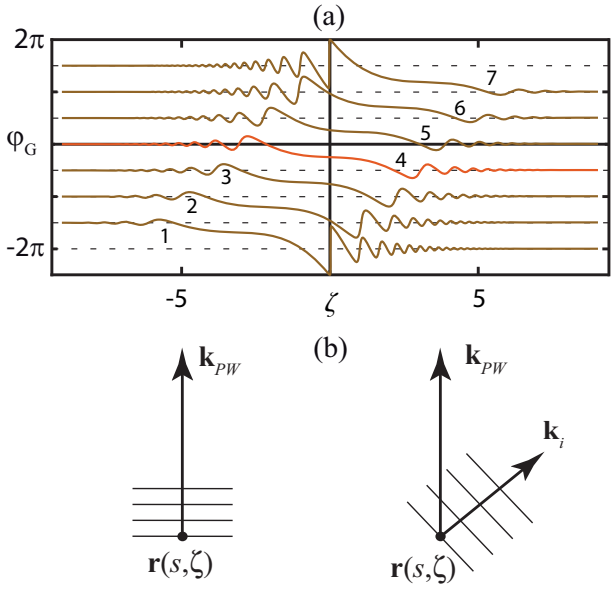

Fig. 2. (a) GP for $k = \{0, \pm 0.41, \pm 1.00, \pm 1.52\}$. The curves are displaced by $\pi/2$ from one to another, with increasing k down upward. The numbers code agrees with that applied in Fig. 1. (b) Geometrical interpretation of the GP in terms of the local wave vector $\vec{k}_{PW}$ of a plane wave and that $\vec{k}_i$ of a paraxial beam.

This effect is not caused by the finite energy of the beam since it is observed for $a = 0$, but it occurs by a non-even symmetry of its spatial spectrum (2).

In the far field, however, the behavior of the AiB is completely different. Applying the PSP, no more than one spatial frequency k is of relevance. The resultant Fraunhofer pattern is $u \to (2\pi i\zeta)^{-1/2}\,\tilde{u}(k)u_{PW}(s,\zeta)$, valid in the limit $|\zeta| \gg k_{max}$ for points of the contour $C \equiv s = k\zeta + a^2 - k^2$ taken from Eq. (3). Note that the paraxial wave field $u_{PW} = \exp\left(iks - ik^2\zeta/2\right)$ corresponds to a non-truncated plane wave.

3. The Gouy phase

Let us go back with the evaluation of the GP in AiBs. The GP $\varphi_G(\zeta)$ is commonly estimated as the cumulative phase difference between a given paraxial field and a plane wave also traveling in the $+z$ direction [4]. Considering a centrosymmetric distribution of u around $s = 0$, the dephase $\varphi_G(\zeta)$ may be derived analytically as the difference $\phi(\zeta) - \lim_{\zeta\to-\infty}\phi$ evaluated along the beam axis. Due to the particular acceleration of the AiB, however, one cannot encounter a beam axis in this case.

In a more general approach, the GP might account for dephasing between the wave field u given in (1) and a plane wave $u_{PW} = \exp(i\psi)$ with a given tilt $k \neq 0$. Following the discussion given above, the phase fronts of u and u_{PW} become parallel in the far field around the light ray (3). In order to obtain $\varphi_G(\zeta)$ for the normalized angle k we employ $\phi - ks + k^2\zeta/2$ instead of ϕ, which is now evaluated at points of the contour C. In Fig. 2(a) we plot $\varphi_G(\zeta)$ for different values of the zenith angle k. As expected, the value of the GP varies rapidly in the near field. Well beyond the near field, in the limit $\zeta \to +\infty$, the GP shift approaches $-\pi/2$.

#172359 - $15.00 USD Received 10 Jul 2012; revised 6 Aug 2012; accepted 6 Aug 2012; published 28 Sep 2012

4. Physical interpretation

Let us give a physical interpretation of our approach, which in principle may be applied to any finite-energy wave field that lacks a beam axis. For that purpose, it is illustrative to rewrite the GP as the line integral

$$\varphi_G(\zeta) = \int_C \Delta\vec{k}\cdot d\vec{r}, \tag{5}$$

where $\Delta\vec{k} = \nabla\phi - \nabla\psi$ and C represents a contour of integration (3) with startpoint at $\zeta \to -\infty$. The form is exactly the same as that encountered when we calculate the work done by a resultant *force* $\Delta\vec{k}$ that varies along the path C. Here $\Delta\vec{k}$ is understood as the difference of the local wave vector $\vec{k}_i = k_0\hat{z} + \nabla\phi$ of the AiB and that corresponding to the reference plane wave, $\vec{k}_{PW} = k_0\hat{z} + \nabla\psi$. Note that $\vec{k}_{PW}$ approaches $k_0\hat{z} + (k/w_0)\hat{x}$ to order k, and that $\vec{k}_{PW} \parallel d\vec{r}$ over the contour C. This is of relevance since many physical processes, like the generation of curved plasma channels [13] and the optical manipulation of microparticles [12], depends openly on $\vec{k}_i$, which is in direct proportion to the electromagnetic momentum and the time-averaged flux of energy [20].

Going from $\vec{r}$ to $\vec{r} + d\vec{r}$ over C leads to a nonnegative contribution of the line integral (5) if (a) the wave vectors $\vec{k}_{PW}$ and $\vec{k}_i$ are nonparallel, and if (b) the wavenumber k_0 of the reference plane wave and that $k_i = |\vec{k}_i|$ of the field u are different. This is illustrated in Fig. 2(b). For a Gaussian beam $\varphi_G = -\pi/4 - \arctan(\zeta)/2$ at $k = 0$, where $\vec{k}_i \parallel \vec{k}_{PW}$ but $k_i < k_0$. In AiBs, however, both angular and modular detuning of $\vec{k}_i$ are produced.

To examine the angular detuning, it is illustrative to represent $\vec{k}_i$ graphically by means of the Poynting vector streamlines (PSLs). Commonly employed with vector fields, the PSLs are tangent to the vector $\vec{k}_i$ and consequently they satisfy the differential equation $\vec{k}_i \times d\vec{r} = 0$, that is $dx/dz = (\vec{k}_i\cdot\hat{x})/(\vec{k}_i\cdot\hat{z})$. The PSLs indicate the direction of wave propagation since they are perpendicular to the phase fronts. Under the paraxial approximation the equation for the PSLs reduces to $ds/d\zeta = \partial_s\phi$ in normalized coordinates. For an AiB we finally have

$$\frac{ds}{d\zeta} = \frac{\zeta}{2} + \mathrm{Im}\frac{Ai'\left(s - \zeta^2/4 + ia\zeta\right)}{Ai\left(s - \zeta^2/4 + ia\zeta\right)}, \tag{6}$$

where $Ai'(\alpha) = \partial_\alpha Ai(\alpha)$. The exact solution $s = s_0 + \zeta^2/4$ is obtained for $a = 0$.

Some PSLs of our AiB are drawn in solid lines in Fig. 3(a) and 3(b). In contrast with the trajectories C of light rays (dashed lines), the PSLs hold $ds/d\zeta = 0$ at $\zeta = 0$. Therefore, PSLs approach a parabola $s = s_0 + s_0''\zeta^2/2$ in the neighbourhood of the beam waist, where $s_0'' = as_0 - aAi'(s_0)^2/Ai(s_0)^2 + 1/2$. If $a \ll 1$ and $s_0 \geq 0$ then $s_0'' \approx 1/2$ featuring a regular parabolic trajectory. However for sufficiently large values of $-s_0 \gg 1$ then $s_0'' < 0$ revealing a concavity inversion along the semi-axis. Moreover, in the far field $ds/d\zeta \to k$ leading to exact solutions in the form of Eq. (3) as $|\zeta| \to \infty$. These straight lines represent the asymptotes of the PSLs.

Finally we analyze the modular detuning of the local wave vector with respect to k_0. In fact, modular detuning of $\vec{k}_i$ implies a local deviation of the phase velocity $v_i = \omega/k_i$ with respect to the speed of light $c = \omega/k_0$ in vacuum [19]. Taking into account the paraxial regime, the local wavenumber is given by $k_i = k_0 + \kappa/z_R$, where

$$\kappa = \partial_\zeta\phi + (\partial_s\phi)^2/2. \tag{7}$$

Moreover we may obtain a simple expression for v_i by using $\Delta v/c \approx -\Delta k/k_0 = -\kappa/k_0 z_R$, where $\Delta v = v_i - c$ and $\Delta k = k_i - k_0$. In Fig. 3 we plot the parameter κ operating as a trend indicator of the spatial variation of the phase velocity of the AiB depicted in Fig. 1. In the far field κ vanishes leading to a wave field with wavenumber $k_i = k_0$ and phase velocity $v_i = c$.

#172359 - $15.00 USD Received 10 Jul 2012; revised 6 Aug 2012; accepted 6 Aug 2012; published 28 Sep 2012

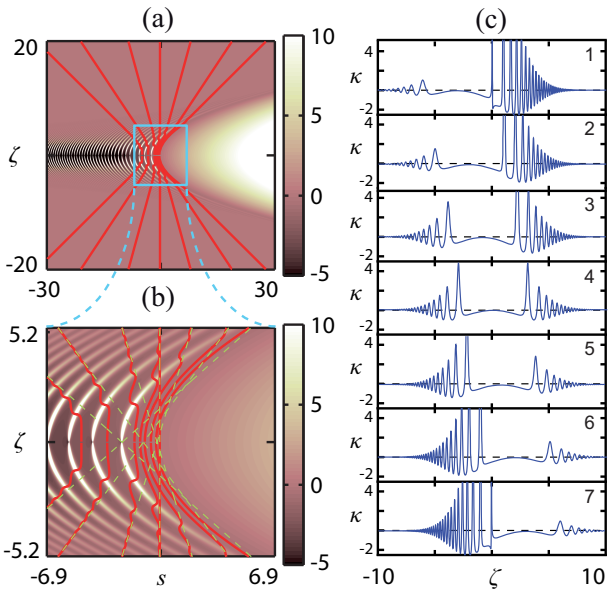

Fig. 3. Spatial distribution of κ and several PSLs for the AiB of Fig. 1. (c) Plots of κ over the numbered contours also representing asymptotes of the PSLs.

However κ presents a more complex behavior in the near field. Out of the geometrical shadow, $\kappa < 0$ and it drops near the peaks of intensity. This effect is associated with superluminality, which is well known in Gaussian beams and other kind of focused beams [21, 22]. Over the caustic of the AiB, however, $\kappa \approx 0$ and it strictly vanishes if $a = 0$. On the contrary, κ grows sharply around the valleys of intensity, and for $a = 0$ it diverges due to the presence of phase singularities.

5. Conclusions

In conclusion, we have rewritten the Gouy phase as a line integral, whose form is exactly the same as that encountered when we calculate the work done by a resultant *force* $\Delta\vec{k}$ that varies along the given path. Here $\Delta\vec{k}$ is understood as the difference of the local wave vector of the AiB, which is in direct proportion to the electromagnetic momentum and the time-averaged flux of energy, and that corresponding to the reference plane wave. The equations describing the Poynting vector streamlines and the spatial variation of the phase velocity for these beams provide a general platform for exploring the flow of electromagnetic energy. These ideas can be used for a variety of applications. For example, our procedure facilitates a means to optically control the movement of particles in air and fluid [12], enabling precision calibration of the direction of forces exerted over trapped objects. In the case of the curved filaments produced in gases by self-bending AiBs [13], the forward emissions coming from different points and propagating along angularly resolved trajectories might be derived in a simple manner with extremely-high accuracy. As such, we envision that the work presented here will add a broad understanding to this new emerging field.

Acknowledgments

This research was funded by the Spanish Ministry of Economy and Competitiveness under the project TEC2009-11635.

#172359 - $15.00 USD Received 10 Jul 2012; revised 6 Aug 2012; accepted 6 Aug 2012; published 28 Sep 2012